Automatic segmentation of intracranial arteries and veins in four-dimensional cerebral CT perfusion scans

Adriënne Mendrik[a)]
Image Sciences Institute, University Medical Center Utrecht, Heidelberglaan 100, 3584 CX, Utrecht, The Netherlands

Evert-jan Vonken
Department of Radiology, University Medical Center Utrecht, Heidelberglaan 100, 3584 CX, Utrecht, The Netherlands

Bram van Ginneken[b)]
Image Sciences Institute, University Medical Center Utrecht, Heidelberglaan 100, 3584 CX, Utrecht, The Netherlands

Ewoud Smit and Annet Waaijer
Department of Radiology, University Medical Center Utrecht, Heidelberglaan 100, 3584 CX, Utrecht, The Netherlands

Giovanna Bertolini
"San Marco" Private Veterinary Clinic, Via Sorio 114/c, 35141, Padua, Italy

Max A. Viergever
Image Sciences Institute, University Medical Center Utrecht, Heidelberglaan 100, 3584 CX, Utrecht, The Netherlands

Mathias Prokop[c)]
Department of Radiology, University Medical Center Utrecht, Heidelberglaan 100, 3584 CX, Utrecht, The Netherlands

(Received 9 October 2009; revised 29 March 2010; accepted for publication 29 March 2010; published 27 May 2010)

Purpose: CT angiography (CTA) scans are the current standard for vascular analysis of patients with cerebrovascular diseases, such as acute stroke and subarachnoid hemorrhage. An additional CT perfusion (CTP) scan is acquired of these patients to assess the perfusion of the cerebral tissue. The aim of this study is to extend the diagnostic yield of the CTP scans to also include vascular information.

Methods: CTP scans are acquired by injecting contrast material and repeatedly scanning the head over time. Therefore, time-intensity profiles are available for each voxel in the scanned volume, resulting in a 4D dataset. These profiles can be utilized to differentiate not only between vessels and background but also between arteries and veins. In this article, a fully automatic method is proposed for the segmentation of the intracranial arteries and veins from 4D cerebral CTP scans. Furthermore, a vessel enhanced volume is presented, in which the vasculature is highlighted and background structures are suppressed. Combining this volume with the artery/vein segmentation results in an arteriogram and a venogram, which could serve as additional means for vascular analysis in patients with cerebrovascular diseases. The artery/vein segmentation is quantitatively evaluated by comparing the results to manual segmentations by two expert observers.

Results: Results (paired two-tailed t-test) show that the accuracies of the proposed artery/vein labeling are not significantly different from the accuracies of the expert observer manual labeling (ground truth). Moreover, sensitivity and specificity of the proposed artery/vein labeling, relative to both expert observer ground truths, were similar to the sensitivity and specificity of the expert observer labeling compared to each other.

Conclusions: The proposed method for artery/vein segmentation is shown to be very accurate for arteries and veins with normal perfusion. Combining the artery/vein segmentation with the vessel enhanced volume produces an arteriogram and a venogram, which have the potential to extend the diagnostic yield of CTP scans and replace the additional CTA scan, but could also be helpful to radiologists in addition to the CTA scan. [DOI: 10.1118/1.3397813]

Key words: segmentation, 4D, arteries, veins, vessels, CT perfusion

I. INTRODUCTION

The use of cerebral computed tomography perfusion (CTP) imaging is increasing rapidly. It is minimally invasive, widely available, and fast.[1–3] Its main current use is to construct perfusion maps of the cerebral tissue, showing cerebral blood volume (CBV), mean transit time (MTT), and cerebral blood flow (CBF) (Ref. 4) in patients with cerebrovascular diseases such as acute stroke,[3,5,6] subarachnoid hemorrhage,[7] and carotid occlusive disease.[8] Of these patients, an additional CT angiography (CTA) scan is usually acquired to assess the vasculature. Therefore, segmentation of cerebral vessels has so far been done on CTA scans.[9–13] CTP scans are routinely reconstructed with 5 mm thick slices to reduce noise in the perfusion maps, which is insufficient for vessel analysis. For this study, 0.625 mm slices were reconstructed, resulting in a CTP scan resolution similar to CTA scans, enabling vessel analysis. Although both CTA and CTP require injection of a contrast material, in CTA a volume is scanned at one point in time aiming at either maximum arterial or sometimes venous enhancement, while in CTP several volumes are acquired over time imaging both arterial and venous enhancement. The radiation dose used per temporal CTP volume is lower than the radiation dose used for the CTA volume. Therefore, each temporal CTP volume contains substantially more noise than the CTA volume. This noise level can be reduced, however, by using a combination of the temporal CTP volumes. Furthermore, the time-intensity profiles provided by the 4D CTP scans cannot only be used to distinguish between vessels and background but also between arteries and veins. Once arteries and veins are segmented, these segmentations could be employed to construct an arteriogram and a venogram from the CTP scan, potentially replacing the CTA scan, thereby reducing costs and total radiation dose to the patient. A limitation of the CTP scan, however, is that the scan coverage is limited to the detector width of the scanner. The 64-slice scanner used for this study has a 4 cm coverage, while CTA scans have a much larger coverage. Newer scanners[14–18] are able to acquire CTP scans with whole brain coverage, solving this limitation.

Not much work has been published so far on the separation of cerebral arteries and veins in thin-slice 4D CTP scans. In a recent paper by Gratama van Andel *et al.*,[19] a method was proposed to obtain CTA images from CTP scans by using weighted averaging and masking to suppress bone and veins. The method is semiautomatic since at least one volume of interest (VOI) has to be set in one of the cerebral arteries or veins to determine the weights for averaging. One of the drawbacks of this method is that the enhancement of arteries or veins depends highly on the selected VOI. Moreover, bone masking in the final CTA image (threshold and dilation) might remove part of the vessels located in close proximity to the bone. To reduce noise, 1.25 mm thick slices were used instead of the available 0.625 mm thick slices. The method was applied to eight datasets, but the quality of artery/vein separation was not evaluated.

Other methods for separating arteries and veins proposed in literature were applied to magnetic resonance (MR) scans. Bock *et al.*[20] proposed a method to separate pulmonary arteries and veins based on the correlation of the signal-time curves in multiphase contrast-enhanced MRA data. User interaction is required to indicate a region of interest (ROI) within an artery and a vein for determining the reference curves for correlation. The authors found that the quality of separation was dependent on the location of the ROI. This method was applied to five datasets, but no quantitative evaluation of the artery/vein separation was performed. Lei *et al.*[21] proposed a semiautomatic method for separating arteries from veins on MR angiography (MRA) data using fuzzy connectedness. The method is semiautomatic since a user has to specify seed voxels in major artery and vein branches. Another semiautomatic method on MRA was proposed by van Bemmel *et al.*,[22] where a level-set based approach is used. A central arterial and venous axis is determined by the minimum-cost path between two (or more) user specified points. These central axes are used as initialization for evolving the arterial and venous level sets. The last two methods both use spatial connectedness and not temporal information to separate arteries and veins.

Vendor CTP software packages offer vessel segmentation to eliminate vessels in the perfusion maps by setting a threshold on the cerebral blood volume (CBV) map since vessels show high CBV values. Kudo *et al.*[23] determined that the best vascular pixel-elimination threshold for thick-slice (4 or 8 mm) CTP data is 8 ml/100 g. Using this threshold on thin slice (0.625 mm) CTP data, however, will include a large part of the parenchyma due to the high noise level in these thin slice scans. At least one vendor offers dynamic CTA volumes from CTP scans.[14,15,17,18,24] The CTA volumes are created by subtracting the first temporal volume from each temporal volume in the CTP scan. Therefore, the first temporal volume is often scanned with a higher dosage (300 mA s) than the rest of the temporal volumes (100 mA s).[18] Subtraction of the first temporal volume decreases the signal to noise ratio (SNR) of the dynamic CTA volumes. Siebert *et al.*[15] found that the image quality of the intracranial 4D 320-slice CTA images was significantly inferior to that of the 3D CTA. Although both the arterial and venous phase can be viewed, there is no strict separation of arteries and veins in these images. In the arterial phase, for example, the veins could already be partially filled with the contrast material even though the peak enhancement has not been reached yet, obscuring the view on the arteries. Dynamic CTA can, however, be helpful in assessing hemodynamics.[24]

In this paper, a fully automatic method is proposed for the segmentation of arteries and veins on 4D cerebral CT perfusion scans. The novelty of the proposed method is twofold. First, a vessel enhanced volume is extracted from the 4D CTP scan, suppressing background structures without affecting the vessel walls, thereby presenting a clear view on the vasculature. Second, no user interaction is required for separating arteries and veins. Temporal information within the vessel segmentation is utilized to automatically classify voxels as artery or vein. A quantitative evaluation of the artery/vein segmentation is performed by comparing the results of

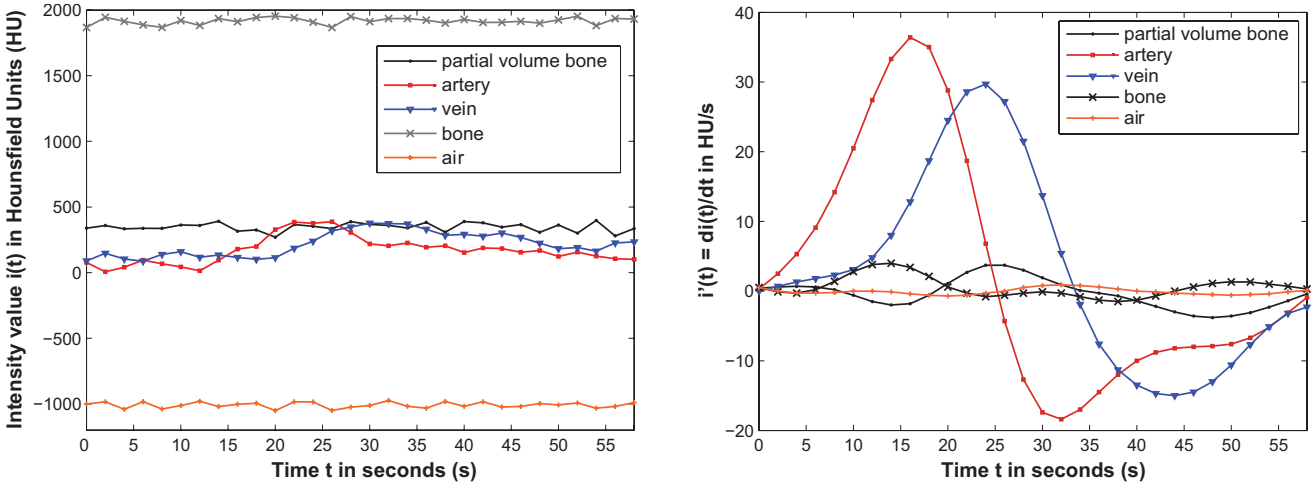

(a) Time-intensity profiles i(t) (b) First Gaussian derivative profiles di(t)/dt

FIG. 1. Illustration of the CTP time-intensity profiles and their first Gaussian derivative profiles. The scale (σ) of the first temporal Gaussian derivative was set to be 6 s. Static structures (bone and air) show minor intensity change over time and can be well separated in (b) from the vessels (artery and vein) with a large intensity change over time. Notice that at $t=24$ s in (a) the artery has a similar intensity value as the partial volume bone, which is problematic for vessel segmentation in CTA (e.g., near the skull base).

the proposed method to manual segmentations of arteries and veins within specified regions of interest by two expert observers.

II. METHOD

The proposed method consists of several steps, which will be described in this section. CTP scans are composed of multiple volumes acquired over time and are therefore prone to head movement. Since this will disturb 4D analysis, registration of the time volumes is an essential preprocessing step for further analysis (Sec. II A). In order to detect the vasculature in the 4D CTP data, a vessel enhanced volume is extracted (Sec. II B) from which the intracranial vessels are segmented (Sec. II C). Finally, arteries and veins are separated within the vessel segmentation to arrive at an arteriogram and a venogram (Sec. II D).

II.A. Registration

Cerebral CTP scan volumes can be registered using 3D rigid registration, assuming that nonrigid movement of intracranial structures during acquisition is negligible. The skull is used for registration, being rigid and simple to mask by setting a threshold at 600 Hounsfield units (HU) and selecting the largest connected component in each time volume. A threshold of 600 HU was selected to exclude vessels connected to the skull in the contrast-enhanced time volumes. Registration was performed using the sum of squared differences as a similarity measure and a gradient descent algorithm to solve the optimization problem [with ELASTIX, a registration package freely available at elastix.isi.uu.nl (Ref. 25)]. All temporal volumes were registered to the first volume. Due to registration, some temporal volume areas could move outside the field of view, causing discontinuities in the time-intensity profiles of some voxels within the field of view. In this method, only voxels with complete time-intensity profiles are used for further processing. However, up to a certain extend, interpolation could also be employed to restore the missing intensity values.

II.B. Vessel enhancement

In CTP scans, the vasculature shows a large intensity change over time due to injection of the contrast material, resulting in a contrast enhancement curve. On the other hand, structures like bone and air show a static intensity value over time, apart from noise [Fig. 1(a)]. In 3D CTA scans acquired at one point in time, the intensity values of the vasculature partially overlap with the intensity values of partial volume bone [Fig. 1(a), $t=24$ s artery curve]. This is especially problematic with vessels located in close proximity to the bone. For vessel segmentation purposes in CTA, bone can be eliminated by registering an unenhanced CT scan of the same patient to the CTA scan, in which the bone can simply be segmented.[9] A similar method is used for CTP scans by Gratama van Andel *et al.*,[19] with the difference that the unenhanced scan is already present in the CTP scan as the first time volume, and thus bone is segmented in this volume. The method proposed in this paper, however, uses the complete time-intensity profiles available in CTP scans to enhance the vasculature and suppress background structures. The first Gaussian derivative is known for its ability to detect edges in noisy images.[26] These edges are essentially large intensity changes. Since the first Gaussian derivative has the ability to detect edges in noisy images, it could also be used to detect contrast in noisy vascular contrast enhancement curves, which show a large intensity change over time. The scale (σ of the Gaussian) of the first temporal Gaussian derivative was set to be 6 s and was selected based on prior experiments to result in the largest contrast between background noise and vascular signal. Figure 1(b) illustrates the enhancement

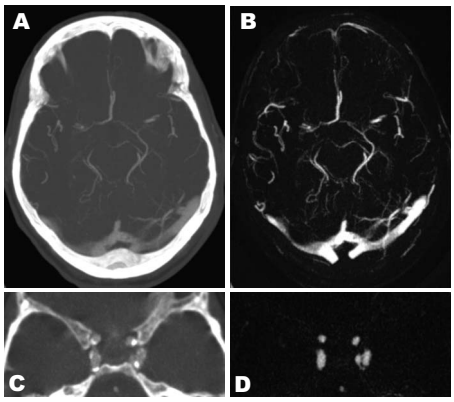

FIG. 2. [(a) and (b)] MIP slab (12 mm) of temporal MIP (window: 2120 HU; level: 460 HU) of the original 4D CTP scan (a) and vessel enhanced volume (window: 570 HU; level: 300 HU) (b). [(c) and (d)] One slice of the temporal MIP (window: 1190 HU; level: 430 HU) of the original 4D CTP scan at the skull base showing partial volume bone and vessels with similar intensity (c) and vessel enhanced volume (window: 520 HU; level: 290 HU) showing only vessels and background (d).

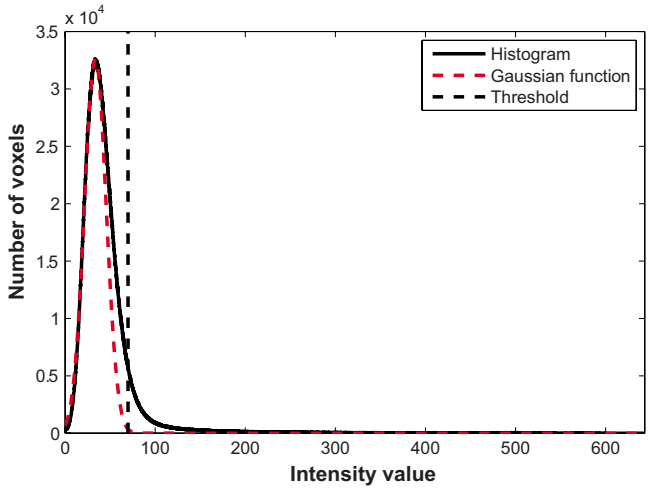

FIG. 3. Histogram of a vessel enhanced volume extracted from a CTP scan. A Gaussian distribution is placed over the left part of the histogram (background noise). Vessel segmentation was performed by setting a threshold at 3σ on the right side of the Gaussian distribution, assuming that all gray values above this threshold belong to vessels, not background.

of the artery and vein curves in contrast to the curves of static structures such as bone and air. The first temporal derivative shows the amount of intensity change at each point in time, and its sign represents the direction of this change. Therefore, to quantify the amount of intensity change during the acquisition, the absolute area under the first temporal derivative curve is determined. Since vessels show a large intensity change over time, this is done for each voxel in the image to create the vessel enhanced volume using the trapezoidal rule,

$$\int_{t=0}^{T-1} |i'(t)|dt = \sum_{t=0}^{T-1} \frac{1}{2}(|i'(t)| + |i'(t+1)|), \quad (1)$$

where $i'(t)=di(t)/dt$ and T is the duration of the acquisition sequence. Figure 2(b) shows an example of a maximum intensity projection (MIP) slab of a vessel enhanced volume. To illustrate suppression of the partial volume bone at the skull base, Fig. 2(d) shows one slice of the vessel enhanced volume zoomed in on the skull base.

II.C. Vessel segmentation

The vessel enhanced volumes extracted from the CTP scans show both arteries and veins. Most vessel segmentation methods for 3D images segment the arteries (for example, in CTA or MRA). They are generally based on assumptions such as the tubular shape of the vessel and the fact that the vasculature is a treelike structure. Arteries have a tubular shape (circular cross section) due to the large amount of muscle in their thick walls and the high pressure on the wall. Veins, however, have thinner walls, and because the walls are collapsible, they may change shape, depending on the surrounding tissue conditions. For example, the cross section of the cavernous, superior sagittal, and transverse sinuses are generally not circular, while the cross section of some smaller veins appear to be more circular. Furthermore, some arteries and veins are located in close proximity to one another, which complicates separation based on shape. Another limitation is that CTP scans acquired on a 64-slice scanner do not contain the complete arterial and venous tree due to limited coverage, whence not all arteries and veins are connected to each other. In the method proposed in this paper, the vessel segmentation (both arteries and veins) is performed on the vessel enhanced volume.

Although nonrigid movement of the intracranial structures is negligible, nonrigid movement of extracranial structures (such as skin, ears, and the head relative to the cushion) is not. These structures give a false signal in the vessel enhanced volume and therefore need to be masked out. This is done by extracting a skull mask and using the outer border of the skull mask as seeds for region growing toward the borders of the image on each slice in the volume.

Since the extracranial structures are removed and the intracranial nonvascular structures are suppressed in the vessel enhanced volume, a threshold can be used to segment the vessels. In this way, no vessels are excluded due to nonconnectivity to a seed voxel or nontubular shape. The threshold is based on the histogram (bin size=1 HU) of the masked vessel enhanced volume. Assuming that the first part of the histogram is background noise with a Gaussian distribution, a Gaussian function is placed over the left side of the histogram peak. The mean μ of the Gaussian function is the intensity value at the histogram peak and the standard deviation $\sigma=\omega/2\sqrt{2\ln 2}$, with ω as full width at half maximum on the left side of the histogram peak. The threshold is set beyond the background noise at $\mu+3\sigma$ (see Fig. 3).

II.D. Artery/vein segmentation

The last step of the proposed method is to separate the arteries from veins within the vessel segmentation. The arterial contrast enhancement curve shows an earlier time to peak (TTP) than the venous contrast enhancement curve

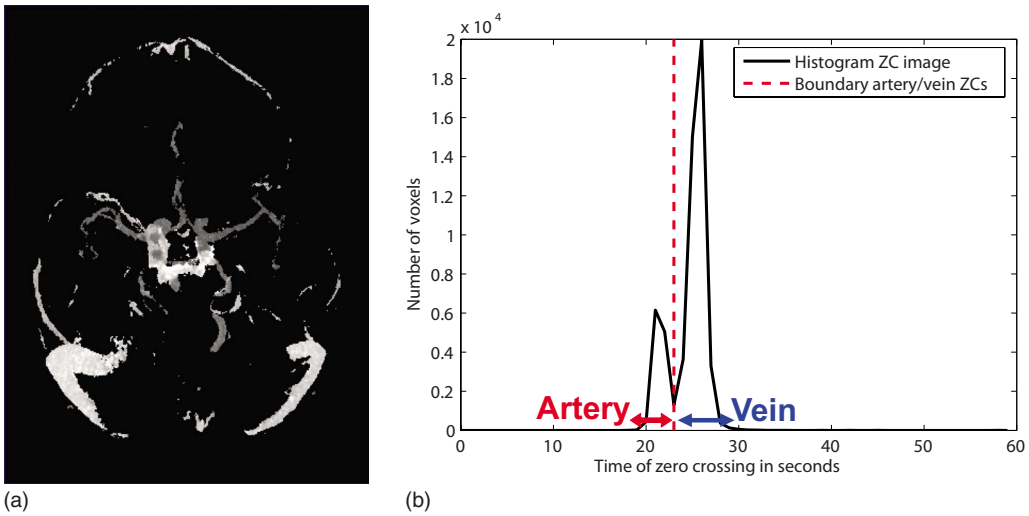

FIG. 4. (a) Maximum intensity projection of an eroded version (structure element: Sphere; kernel half size: 2) of the ZC image. Low intensity areas show an earlier ZC than high intensity areas. (b) Histogram of the eroded ZC image, showing an arterial and a venous peak. Voxels with a ZC within the arterial peak are assigned to the artery segmentation and voxels with a ZC within the venous peak to the vein segmentation.

[Fig. 1(a)] as blood flows from the arteries, via the parenchyma, to the veins. This information is employed to separate the arteries from the veins.

The zero crossing (ZC) of the first temporal Gaussian derivative ($i'(t)$) curve [Fig. 1(b)] corresponds to the TTP of the contrast enhancement curve after a Gaussian smoothing with a σ of 6 s. Since the first temporal Gaussian derivative was already determined to construct the vessel enhanced volume, the zero crossings are used to determine the TTP. First the highest peak of the $i'(t)$ curve is detected and a forward search is used to detect two points t_1 and t_2, where $i'(t_1)>=0$ and $i'(t_2)<=0$. A linear approximation between these points is used to retrieve the zero crossing (ϕ): $\phi=-b/a$ with $a=(i'(t_2)-i'(t_1))/(t_2-t_1)$ and $b=i'(t_2)-(a\cdot t_2)$. A zero crossing image is created, which shows the zero crossings of each voxel within the vessel segmentation. To determine the arterial zero crossings and venous zero crossings, the histogram of an eroded version (structure element: Sphere; kernel half size: 2) of the zero crossing image is used. This selects the larger arteries and veins [Fig. 4(a)]. The two highest peaks in the histogram are detected: The first corresponding to the arterial peak and the second to the venous peak. The separation between arterial and venous zero crossings is set to be the minimum between these two peaks in the histogram [Fig. 4(b)]. The outer borders are located at the point where the histogram reaches zero, searching backward from the arterial peak and forward from the venous peak. Voxels with an arterial zero crossing within the vessel segmentation were labeled as artery, and voxels with a venous zero crossing were labeled as vein. To remove background noise from the segmentation, connected components (connectivity 26) with less than 20 voxels were discarded in both the artery and the vein segmentation [Figs. 6(b) and 6(d)]. From these segmentations, an arteriogram and a venogram can be constructed by suppressing either the veins or the arteries in the vessel enhanced volume [Figs. 6(c) and 6(e)].

III. EXPERIMENTS

The proposed method was applied to 20 patient cerebral CTP scans (scanned every 2 s during 60 s at 80 kVp and 150 mA s), acquired on a Philips Brilliance 64-slice CT scanner during injection of 40 ml of (300 mg I/ml) contrast agent at 5 ml/s and reconstructed with 0.625 mm thick sections.

Patient scans were selected consecutively from our database, but only scans that included the Circle of Willis area were selected. Postoperative subarachnoid hemorrhage patient scans were excluded, as well as patient scans with large metal artifacts, since the vasculature was obscured by these artifacts and could not be assessed. The evaluation data consisted of 15 patients with subarachnoid hemorrhage, 3 with carotid occlusive disease, and 2 with acute stroke. The Institutional Review Board of the University Medical Center Utrecht approved our retrospective study, and informed consent was waived.

III.A. Quantitative experiments

To allow for quantitative evaluation, arteries and veins were manually labeled by two expert observers within 20 ROIs in each of the 20 CTP scans. The 2D ROIs (rectangles in Fig. 7) were drawn by one of these observers to include clinically relevant arteries and veins on several axial slices throughout the scan. A combination of anatomical knowledge and temporal information (contrast enhancement over time) was used to distinguish between arteries and veins. Manual labeling was performed on a temporal maximum intensity projection of three time points to increase vessel visibility in the 4D CTP dataset. The observers were instructed to scroll back and forth through the temporal dimension to make sure that both arteries and veins were labeled. The labeling was performed on the original 4D CTP datasets after registration. Two experienced observers first labeled the arteries and veins, after which the expert observers checked and corrected their labels.

A manual segmentation tool was developed, in which a red label indicated artery voxels, a blue label indicated vein voxels, and a yellow label indicated vessel voxels of which the observers were not sure if it was artery or vein. Drawing artery and vein voxels could be done on a per voxel level or using various larger brush sizes. Owing to partial volume, determining the exact borders of the vessels is a difficult task. To simplify the segmentation, a smart brush was included, which clipped the segmentation to the vessel border using optimal thresholding, after which the observer could manually correct the segmentation if not satisfied with the result. For the expert observers, an extra option was available to correct whole segments to red or blue.

After having applied the proposed segmentation method to the 20 cerebral CTP scans, the automatic segmentations were compared to the manual segmentations, and accuracy, specificity, and sensitivity were determined. Both observers were consecutively used as ground truth and were compared to each other. To validate the method of letting the expert observers check and correct labels set by experienced observers, 5 out of the 20 patient scans were additionally labeled by the expert observers without prelabeling by the experienced observers. Accuracy, specificity, and sensitivity were determined compared to the initial prelabeled segmentations of these five scans.

III.B. Qualitative experiments

Routinely CBV maps are constructed from the thick-slice (5 mm) CTP scans. These maps could also be created from the thin-slice (0.625 mm) CTP data, which would be another method to show the vasculature. Determining the CBV requires the detection of a baseline, which is sensitive to noise, and the fitting of a function (for example, Gaussian or gamma) over the contrast enhancement curve to exclude the recirculation peak before the area under the curve is determined. For each voxel in the image, the area under the contrast enhancement curve is divided by the area under the curve of a vascular reference pixel,[4] which is routinely manually selected.

A CBV was constructed of one of the patient CTP scans using the brain CT perfusion software of Philips version 4.0. Before constructing the CBV, the data were filtered in the temporal direction using a Gaussian with a σ of 6 s (equivalent to the σ used for the proposed vessel enhanced volume). In this way, both the CBV and the vessel enhanced volume receive at least an equal amount of smoothing. However, additional spatial and temporal filtering was performed by the Philips software prior to determining the CBV.

In most vendor packages vessels in cerebral perfusion maps are eliminated by setting a threshold on the CBV map, which is also a vessel segmentation method. Kudo *et al.*[23] recommended using a threshold of 8 ml/100 g for 4–8 mm slices, which is routinely used in clinical practice. We applied this threshold for vessel segmentation on the CBV map.

Dynamic CTA volumes were constructed to compare the results of the arteriogram and venogram to the arterial and venous phases of these CTA volumes extracted from the CTP scans.[14,15,17,18,24] The CTA volumes were created by subtracting a mask image from the arterial and venous temporal volumes, as described in Salomon *et al.*[18] Since the first temporal volume in these sequences is acquired with a higher dose (300 mA s), we averaged the first three temporal volumes to simulate the high dose volume and subtracted this volume from the arterial and venous phase. The arteriograms and venograms were created by suppressing either the arteries or veins in the vessel enhanced volume using the artery/vein segmentation.

TABLE I. Results of vessel segmentation with respect to both expert observer manual segmentations. All voxels labeled as vessel were regarded as positives and all the remaining (background) voxels within the region of interest as negatives.

Ground truth: Expert observer 1	Specificity	Sensitivity	Accuracy
Proposed method	0.853	0.963	0.867
Expert observer 2	0.978	0.760	0.950
Ground truth: Expert observer 2	**Specificity**	**Sensitivity**	**Accuracy**
Proposed method	0.841	0.963	0.856
Expert observer 1	0.965	0.840	0.950

TABLE II. To validate the method of letting the expert observers check and correct labels set by experienced observers, 5 out of the 20 patient scans were additionally labeled by the expert observers (2nd labeling) without prelabeling by the experienced observers. Accuracy, specificity, and sensitivity were determined compared to the initial prelabeled segmentations of these five scans. All voxels labeled as vessel were regarded as positives and all the remaining (background) voxels within the region of interest as negatives.

Ground truth: Expert observer 1	Specificity	Sensitivity	Accuracy
Proposed method (threshold at 3σ)	0.879	0.972	0.888
Expert observer 1 2nd labeling	0.987	0.748	0.963
Expert observer 2	0.982	0.769	0.960
Expert observer 2 2nd labeling	0.985	0.754	0.961
Ground truth: Expert observer 2	**Specificity**	**Sensitivity**	**Accuracy**
Proposed method (threshold at 3σ)	0.871	0.959	0.879
Expert observer 2 2nd labeling	0.981	0.774	0.961
Expert observer 1	0.974	0.828	0.960
Expert observer 1 2nd labeling	0.979	0.732	0.956

IV. RESULTS

IV.A. Quantitative results

Two steps of the method were evaluated separately. The results of the vessel segmentation are shown in Tables I and II, and the results of the artery/vein labeling are shown in Tables III and IV.

For the vessel segmentation evaluation, all voxels labeled as vessel (red, blue, and yellow labels) were regarded as positives and all the remaining (background) voxels within the ROI as negatives. The proposed vessel segmentation

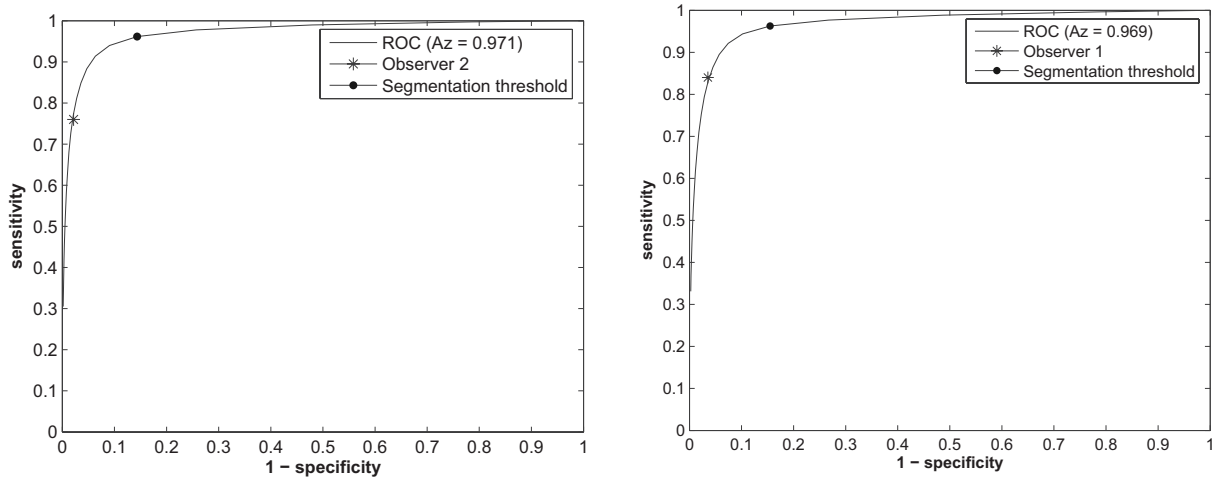

(a) ROC curve, ground truth: Observer 1 (b) ROC curve, ground truth: Observer 2

FIG. 5. ROC curves of shifting the vessel segmentation threshold (see Fig. 3) from -5σ to 20σ on the vessel enhanced volume. The proposed segmentation threshold is located at 3σ. (a) The manual segmentation of observer 1 is used as ground truth. The manual segmentation of observer 2 is located at approximately 9σ on the ROC curve. The area under the ROC curve (Az) is 0.971. (b) The manual segmentation of observer 2 is used as ground truth. The manual segmentation of observer 1 is located at approximately 8σ on the ROC curve. The area under the ROC curve (Az) is 0.969.

method shows a high sensitivity, but a lower specificity and accuracy compared to both expert observers (Table I). This indicates that the proposed method results in an oversegmentation compared to both manual segmentations. This oversegmentation is, however, necessary to completely suppress the arteries and veins for constructing the arteriogram and venogram. Figure 5 shows the receiver operating characteristic (ROC) curves with respect to both observer segmentations. The manual and automatic segmentations are located on either side of the optimal threshold. Figure 6 illustrates that setting the threshold close to the manual segmentation of observer 1 would be insufficient to suppress the complete arteries and veins (including partial volume voxels). Table II shows the results for the five patient scans with additional expert labels.

For the artery/vein segmentation evaluation, only the artery and vein labeled voxels (red/blue) were taken into account. Voxels labeled as artery were regarded as positives and voxels labeled as vein as negatives. A paired two-tailed t-test was performed, comparing the accuracy values per patient of the proposed method to those of the expert observers, of which the results are presented in Table III. The accuracies of the proposed artery/vein labeling are not significantly different from the accuracies of the observers, and the specificity and sensitivity are also similar to those of the observers. Table IV shows the results for the five patient scans with additional expert labels.

Figure 7 shows the results of the segmentation of the proposed method compared to both manual segmentations in ROIs taken from various patients. The temporal maximum intensity projection of the original 4D CTP scan and the

TABLE III. Results of artery/vein labeling with respect to both expert observer manual segmentations. Only the artery and vein labeled voxels were taken into account. Voxels labeled as artery were regarded as positives and voxels labeled as vein as negatives. A paired two-tailed t-test was performed, comparing the accuracy values per patient of the proposed method to those of the expert observer.

Ground truth: Expert observer 1	Specificity	Sensitivity	Accuracy	t-test
Proposed method	0.985	0.928	0.963	0.725
Expert observer 2	0.985	0.936	0.966	–
Ground truth: Expert observer 2	**Specificity**	**Sensitivity**	**Accuracy**	**t-test**
Proposed method	0.964	0.958	0.961	0.467
Expert observer 1	0.961	0.975	0.966	–

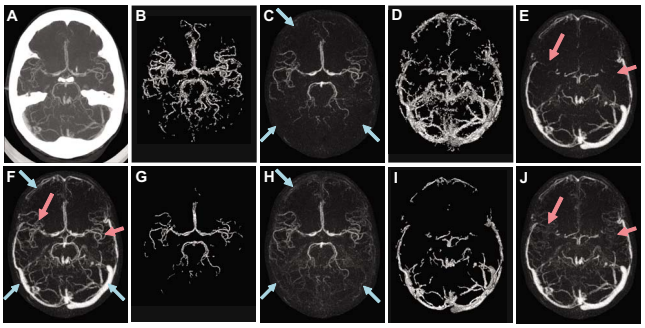

FIG. 6. Illustration of the artery/vein segmentations at 3σ (proposed vessel segmentation threshold) and 8σ [close to manual segmentation of observer 1 in Fig. 5(b)]. (a) shows a MIP of the temporal MIP of the original 4D CTP scan as a reference (window: 660; level: 270). (f) shows a MIP of the vessel enhanced volume (window: 370; level: 210). The threshold at 8σ [isosurface renderings in (g) and (i)] results in an undersegmentation, therefore suppression of arteries and veins in the vessel enhanced volume (f) to create the arteriogram [MIP in (h)] and venogram [MIP in (j)] leaves edges and small vessels indicated by the arrows. The proposed vessel segmentation threshold at 3σ [isosurface renderings in (b) and (d)] results in an oversegmentation, but is better suited for suppression of arteries and veins in the vessel enhanced volume (f) to show the arteries in the arteriogram [MIP in (c)] and the veins in the venogram [MIP in (e)].

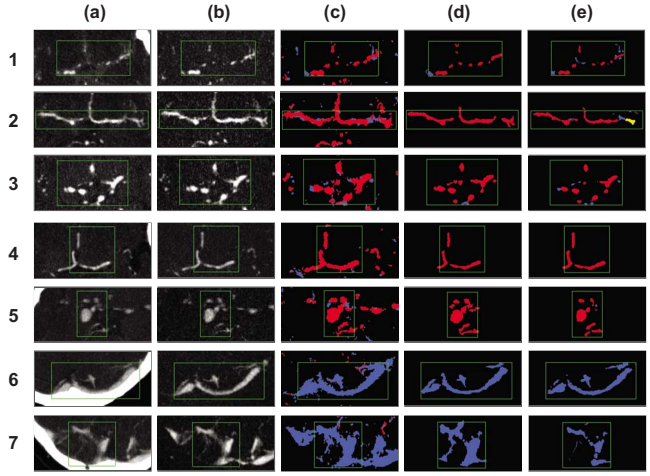

FIG. 7. Illustration of the regions of interest in various patients used for evaluating the proposed method. For each row, (a) shows the temporal maximum intensity projection of the original 4D CTP data, (b) shows the vessel enhanced volume, (c) shows the automatic segmentation of the proposed method, which shows an oversegmentation used for suppressing the arteries and veins in the vessel enhanced volume, (d) shows the manual segmentation of expert observer 1, and (e) shows the manual segmentation of expert observer 2. Rows 1–4 show examples of the Circle of Willis area, which is the most challenging area for separating arteries from veins. Row 5 shows an aneurysm correctly segmented as artery. Rows 6 and 7 show veins located near the skull, illustrating the suppression of the skull and preservation of the vein boundary in the vessel enhanced volume.

vessel enhanced volume are also presented as a reference. The figure shows that vessels of different vessel sizes, ranging from small (≈0.86 mm) to large (≈9 mm), were targeted by the algorithm and contained in the ROI. However, annotating very small vessels in the original 4D data is very challenging for the observers due to the high level of noise in these scans. The total number of voxels labeled is 18.5×10^5 (21.3×10^1 cm^3) of the 12.5×10^7 voxels (14.4×10^3 cm^3) in the brain parenchyma. On average, 1.86% of the total brain parenchyma was annotated per patient scan. Even though the ROIs did not cover a large part of the data, they were well distributed throughout the volume to include diagnostically important arteries and veins, such as the aneurysm in row 5 of Fig. 7. Annotating 4D data is very time consuming since observers need to go up and down through the volume to check the connectivity of vessels and through the temporal direction to check the maximum enhancement for each of the vessels within the ROI.

TABLE IV. To validate the method of letting the expert observers check and correct labels set by experienced observers, 5 out of the 20 patient scans were additionally labeled by the expert observers (2nd labeling) without prelabeling by the experienced observers. Accuracy, specificity, and sensitivity were determined compared to the initial prelabeled segmentations of these five scans. Only the artery and vein labeled voxels (red/blue) were taken into account. Voxels labeled as artery were regarded as positives and voxels labeled as vein as negatives.

Ground truth: Expert observer 1	Specificity	Sensitivity	Accuracy
Proposed method	0.990	0.932	0.967
Expert observer 1 2nd labeling	0.965	0.977	0.971
Expert observer 2	0.988	0.920	0.962
Expert observer 2 2nd labeling	0.993	0.931	0.972
Ground truth: Expert observer 2	**Specificity**	**Sensitivity**	**Accuracy**
Proposed method	0.966	0.951	0.961
Expert observer 2 2nd labeling	0.981	0.962	0.975
Expert observer 1	0.953	0.978	0.962
Expert observer 1 2nd labeling	0.940	0.984	0.958

IV.B. Qualitative results

Figure 8 shows a MIP of both the CBV created with the Philips brain CT perfusion software and the vessel enhanced volume. Even though additional temporal and spatial smoothing is applied by the Philips software prior to the construction of the CBV, the CBV still contains more noise and therefore results in a worse distinction between vessels and background than the vessel enhanced volume.

Figure 9 shows an example of setting a threshold of 8 ml/100 g (as proposed by Kudo *et al.*[23]) on the thin-slice CBV next to the proposed threshold on the vessel enhanced volume for vessel segmentation. The thin-slice (0.625 mm) data used in this research contain much more noise than the 4–8 mm slice data, for which the threshold proposed by Kudo *et al.* was determined. In the vessel enhanced volume, more noise was suppressed than in the CBV. The threshold proposed by Kudo *et al.* contains much more noise than the proposed vessel segmentation method.

Figure 10 shows subimages of the dynamic CTA arterial and venous phase and the corresponding arteriogram and venogram. A mask image is subtracted from the arterial and venous temporal volumes to create the arterial and venous phases.[18] Although this suppresses static structures in the image, such as bone, it also reduces the SNR, decreasing the quality of the vessels (white arrows in Fig. 10). During the

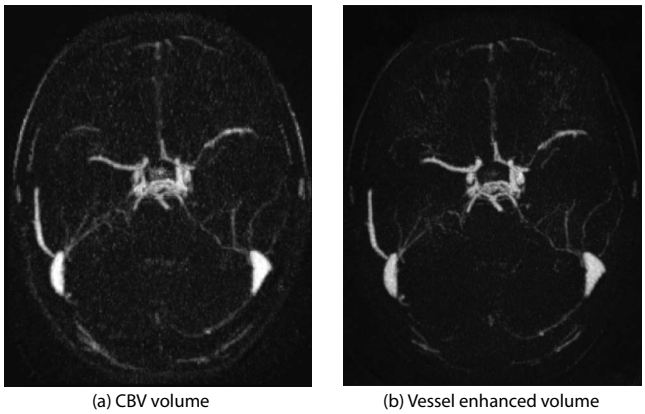

FIG. 8. Illustration of a CBV versus the proposed vessel enhanced volume. The CBV was constructed, after temporal Gaussian smoothing (σ=6 s), using Philips' brain CT perfusion software version 4.0, which performs additional spatial and temporal filtering before determining the CBV. Due to the noise sensitive baseline detection and the use of only part of the temporal sequence, the CBV image is still noisier and gives a worse distinction between vessels and background than the proposed vessel enhanced volume. (a) 13 mm MIP (window: 120; level: 60) of the CBV, (b) 13 mm MIP (window: 570; level: 300) of the proposed vessel enhanced volume.

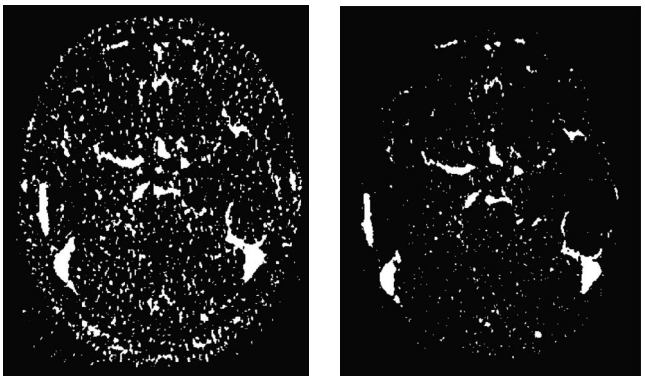

FIG. 9. Illustration of one slice of an 8 ml/100 g threshold on a thin-slice (0.625 mm) CBV (a) and the proposed vessel segmentation threshold on the vessel enhanced volume (b). The 8 ml/100 g threshold was determined by Kudo *et al.* (Ref. 23) to eliminate vessels in 4–8 mm slice data, but the thin-slice (0.625 mm) data used in this research contains much more noise such that part of the parenchyma voxels are also included in the segmentation. Since the vessel enhanced volume contains less noise than the CBV and the proposed threshold was set to be beyond the background noise, the threshold proposed for vessel segmentation contains much less noise than the threshold on the CBV.

arterial phase, some contrast material is already present in the veins, obscuring the view on the arteries (blue arrows in Fig. 10) and during the venous phase some contrast material is still present in the arteries, obscuring the view on the veins (red arrows in Fig. 10). The proposed arteriogram and venogram present a clear view on either arteries or veins.

Figures 11 and 12 illustrate the performance of the proposed algorithm in the presence of artifacts. Figure 11 shows a vessel enhanced volume with the corresponding arteriogram and venogram of a patient CTP scan with an unrecoverable motion artifact. In this case, the patient moved his/her head within the acquisition of one temporal volume such that the scanned temporal volume contained motion artifacts which could not be solved by registration. Although all three images show signal within the skull due to the motion artifact, the arteries and veins are still nicely separated.

Figure 12 shows an example of a metal artifact in a CTA scan with the corresponding vessel enhanced volume. The center of the metal artifact shows static high intensity values over time and is therefore suppressed in the vessel enhanced volume. The borders of the metal artifact are enhanced since these differ per acquired temporal volume. The metal artifact is, however, not more severe on the vessel enhanced volume than on the CTA scan.

To process one patient CTP scan, after registration, takes approximately 12 min on a 2.66 GHz, 64 bit pc with 8 Gbytes of RAM. The algorithm was implemented in C++ and not aggressively optimized for speed.

V. DISCUSSION

In this paper, a fully automatic method for segmentation of arteries and veins on 4D cerebral CTP scans is presented. In 4D analysis of the CTP scans, registration of the temporal volumes is an essential preprocessing step. Errors in the registration can, for instance, cause signal in the vessel enhanced volume at high contrast (bone/air) borders and disturb the time-intensity profiles. However, when the registration quality is sufficient, which is generally the case with rigid registration, the vessel enhanced volume correctly enhances the vasculature and suppresses background structures. An exception arises when unrecoverable motion artifacts are present within one temporal volume, as shown in Fig. 11. Although the image quality decreases due to signal in the skull area, artery/vein separation is still feasible. It can occur, however, that the motion artifacts are too severe for artery/vein separation, in which case the CTP maps (MTT, CBV, and CBF) will also be unreliable. When no motion artifacts are present and the registration quality is sufficient, as shown in the images in rows 6 and 7 of Fig. 7, the bone is clearly suppressed in the vessel enhanced volume, without deterioration of the vessel wall. Compared to the CBV (Fig. 8), the vessel enhanced volume shows more noise reduction even though additional filtering (both spatial and temporal) was performed prior to the creation of the CBV.

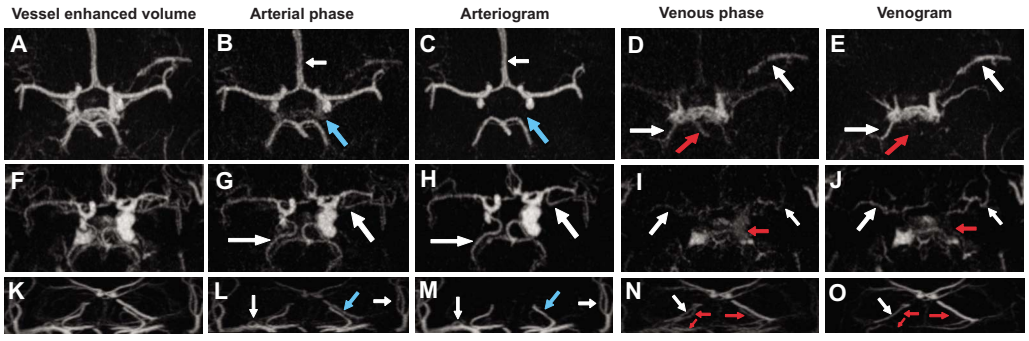

FIG. 10. Subimages of arteriograms and venograms of three patients resulting from either vein or artery suppression in the vessel enhanced volume using the artery/vein segmentation. The arterial and venous phase images are created by subtracting a mask image (average of the first three temporal volumes to simulate a high dose volume) from the arterial and venous temporal volumes Ref. 18). In the arterial and venous phases, the arteries and veins are not strictly separated. Arrows indicate arterial overlap in the venous phase and venous overlap in the arterial phase. The white arrows indicate that the quality of the arteries and veins is less in the arterial and venous phase than that in the arteriogram and venogram. [(a)–(e)] Axial MIP slab of 40 mm (window: 520; level: 320). [(f)–(j)] Axial MIP slab of 45 mm showing an aneurysm (window: 300; level: 450). [(k)–(o)] Coronal MIP slab of 100 mm (window: 410; level: 680).

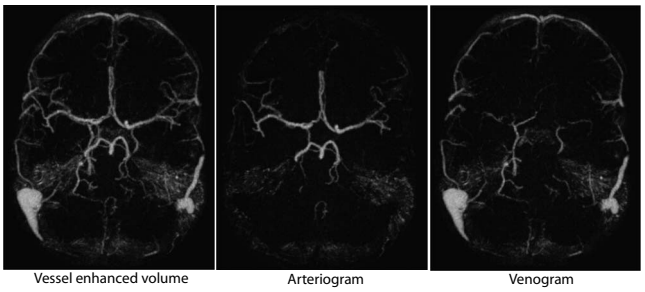

FIG. 11. Illustration of a 35 mm MIP of a vessel enhanced volume (window: 445; level: 285) with the corresponding arteriogram and venogram constructed from a patient CTP scan with unrecoverable motion artifacts (motion within one temporal volume). In this case, the skull also shows signal in the vessel enhanced volume.

Although the proposed vessel segmentation, based on the vessel enhanced volume, results in a better segmentation than setting the threshold proposed by Kudo *et al.*[23] on the thin-slice CBV (Fig. 9), it is an oversegmentation compared to the manual segmentations. Oversegmentation of vessels is not always a drawback of a vessel segmentation method. This highly depends on the purpose of segmentation. For vessel diameter measurements, an accurate localization of the vessel boundary is unquestionably important. The purpose of the proposed vessel segmentation is, however, to function as a rough first segmentation to result in an artery/vein segmentation, which can be used to suppress arteries and veins in the vessel enhanced volume. For suppression of the vasculature, the oversegmentation is, in fact, beneficial. After suppression, using the oversegmentation (3σ), no residual borders are present in the arteriogram and venogram, as shown in Figs. 6(c) and 6(e). Determining the exact border of the vessels is a difficult task due to partial volume and noise, especially in the 4D CTP scans. The ROC curves in Fig. 5 show at which point of the ROC curve the observer segmentation is located. Figures 6(g) and 6(i) show the result of an artery and a vein segmentation with a vessel segmentation threshold close to the manual segmentation of observer 1 (8σ). Using these segmentations for suppressing the arteries and veins fails to suppress the partial volume vessel boundaries and smaller vessels, as shown in Figs. 6(h) and 6(j).

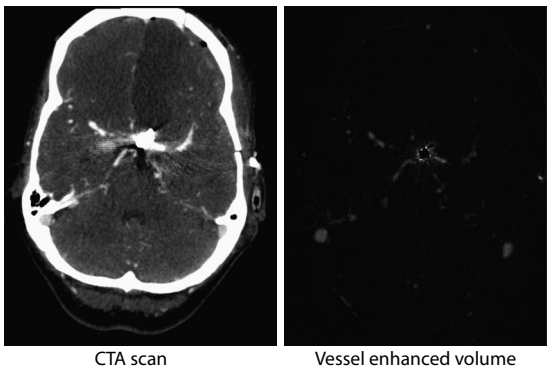

FIG. 12. Illustration of one slice of a CTA scan (window: 330; level: 120) and the corresponding vessel enhanced volume (window: 780; level: 430) showing a metal artifact.

The results of the artery/vein labeling are presented in Table III. The accuracy and specificity of the automatic labeling are similar to both expert observers and the sensitivity is only slightly lower. The paired two-tailed t-test shows that the accuracies of the proposed method are not significantly different from the accuracies of the observers. Although artery/vein labeling evidently works very well in these patients, one should keep in mind that perfusion deficits, as can occur in some acute stroke patients, could influence the artery/vein labeling. Collateral arteries could have a similar time to peak as some veins and could therefore be labeled as veins. These arteries will, however, also be less visible on a CTA scan aimed at the arterial phase. To correct for perfusion deficits, one could think of adding extra rules to the artery/vein separation method. For example, using connectivity in the case of stenoses, or additional shape analysis of the contrast enhancement curve for collaterals in the case of occlusion. In the CTP scans used in this research not all vessels were connected due to limited coverage, and the temporal resolution was too low (2 s) to detect differences in the shape of the contrast enhancement curve. However, since the proposed method for artery/vein separation only uses the TTP to separate arteries from veins, radiologists can use this information to detect collaterals. When collateral arteries are shown in the venogram, radiologists know, based on anatomical knowledge, that these are arteries, but apparently have a similar TTP as the veins, which is typical for collateral arteries. The majority of the patients in this study are subarachnoid hemorrhage patients. These patients suffer from a high risk of having an aneurysm, but perfusion is generally normal. An advantage of the proposed method applied to these patients is that aneurysms are included in the vessel segmentation and correctly labeled as artery, as shown in Fig. 7, row 5.

The manual segmentation method was validated on 5 out of the 20 CTP scans used in the evaluation. The sensitivity, specificity, and accuracy of the second expert observer labeling without experienced observer prelabeling were similar to the first labeling (Tables II and IV). Only the sensitivity of the second labeling of expert observer 1 in Table II (results vessel segmentation) was lower than the first labeling. This means that less voxels were labeled as vessel, which could be due to limited time; the difference is, however, not very large.

The fully automatic artery/vein segmentation combined with the vessel enhanced volume produces the opportunity to display an arteriogram presenting solely the arteries [Fig. 6(c)] and a venogram presenting solely the veins [Fig. 6(e)]. These arteriograms and venograms show a better separation of arteries and veins and better image quality than dynamic CTA images from CTP (Fig. 10). Further research is necessary to investigate whether the quality of these arteriograms and venograms is sufficient to replace the additional CTA scan, thereby reducing cost and radiation dose to the patient. However, these arteriograms and venograms could already

be used in addition to the CTA scan for assessing the vasculature. CTA scans aimed at the arterial phase suffer from venous overprojection (contrast material present in the veins) and other structures such as bone. The arteriograms from CTP present a clear view on the arteries and could be used as a reference. The veins are generally not imaged, but if a CTA scan is acquired aimed at the venous phase, for example, to assess venous thrombosis, bone hampers the view on the larger veins (Fig. 7), which will be solved in the venograms from CTP.

VI. CONCLUSION

Cerebral CTP scans are increasingly being acquired in patients with cerebrovascular diseases. An additional CTA scan is generally acquired to assess the vasculature. In this paper, a fully automatic method is proposed to segment the intracranial arteries and veins from CTP scans. Furthermore, a vessel enhanced volume is presented, which, combined with the artery/vein segmentation, produces an arteriogram and a venogram from CTP. This has the potential to extend the diagnostic yield of CTP scans and replace the additional CTA scan, but could also be helpful to radiologists in addition to the CTA scan. The artery/vein segmentation was quantitatively evaluated by comparing the results to manual segmentations of two expert observers. Results show that the accuracies of the artery/vein labeling were not significantly different from the accuracies of the manual labeling for arteries and veins with normal perfusion.

ACKNOWLEDGMENTS

This work was supported by a research grant from Philips Healthcare. The authors would like to thank Alan Riordan and Hugo de Jong for supplying the CBV map produced by the Philips brain CT perfusion software version 4.0.

[a]Electronic mail: adrienne@isi.uu.nl
[b]Present address: Radboud University Nijmegen Medical Centre, Geert Grooteplein-Zuid 10, 6525 GA Nijmegen
[c]Present address: Radboud University Nijmegen Medical Centre, Geert Grooteplein-Zuid 10, 6525 GA Nijmegen

[1]K. A. Miles, "Brain perfusion: Computed tomography applications," Neuroradiology **46**, s194–s200 (2004).
[2]A. Waaijer, I. C. van der Schaaf, B. K. Velthuis, M. Quist, M. J. P. van Osch, E. P. A. Vonken, M. S. van Leeuwen, and M. Prokop, "Reproducibility of quantitative CT brain perfusion measurements in patients with symptomatic unilateral carotid artery stenosis," AJNR Am. J. Neuroradiol. **28**(5), 927–932 (2007).
[3]M. Wintermark, H. A. Rowley, and M. H. Lev, "Acute stroke triage to intravenous thrombolysis and other therapies with advanced CT or MR imaging: Pro CT," Radiology **251**(3), 619–626 (2009).
[4]E. G. Hoeffner, I. Case, R. Jain, S. K. Gujar, G. V. Shah, J. P. Deveikis, R. C. Carlos, B. G. Thompson, M. R. Harrigan, and S. K. Mukherji, "Cerebral perfusion CT: Technique and clinical applications," Radiology **231**(3), 632–644 (2004).
[5]T. E. Mayer, G. F. Hamann, J. Baranczyk, B. Rosengarten, E. Klotz, M. Wiesmann, U. Missler, G. Schulte-Altedorneburg, and H. J. Brueckmann, "Dynamic CT perfusion imaging of acute stroke," AJNR Am. J. Neuroradiol. **21**(8), 1441–1449 (2000).
[6]M. Wintermark, "Brain perfusion-CT in acute stroke patients," Eur. Radiol. **15**, d28–d31 (2005).
[7]D. G. Nabavi, L. M. LeBlanc, B. Baxter, D. H. Lee, A. J. Fox, S. P. Lownie, G. G. Ferguson, R. A. Craen, A. W. Gelb, and T. Y. Lee, "Monitoring cerebral perfusion after subarachnoid hemorrhage using CT," Neuroradiology **43**(1), 7–16 (2001).
[8]R. Jain, E. G. Hoeffner, J. P. Deveikis, M. R. Harrigan, B. G. Thompson, and S. K. Mukherji, "Carotid perfusion CT with balloon occlusion and acetazolamide challenge test: Feasibility," Radiology **231**(3), 906–913 (2004).
[9]R. Manniesing, B. K. Velthuis, M. S. van Leeuwen, I. C. van der Schaaf, P. J. van Laar, and W. J. Niessen, "Level set based cerebral vasculature segmentation and diameter quantification in CT angiography," Med. Image Anal. **10**(2), 200–214 (2006).
[10]R. Manniesing, M. A. Viergever, A. van der Lugt, and W. J. Niessen, "Cerebral arteries: Fully automated segmentation from CT angiography—A feasibility study," Radiology **247**(3), 841–846 (2008).
[11]H. Shim, D. Kwon, I. D. Yun, and S. U. Lee, "Robust segmentation of cerebral arterial segments by a sequential Monte Carlo method: Particle filtering," Comput. Methods Programs Biomed. **84**(2–3), 135–145 (2006).
[12]M. Hernandez and A. F. Frangi, "Non-parametric geodesic active regions: Method and evaluation for cerebral aneurysms segmentation in 3DRA and CTA," Med. Image Anal. **11**(3), 224–241 (2007).
[13]D. Lesage, E. D. Angelini, I. Bloch, and G. Funka-Lea, "A review of 3D vessel lumen segmentation techniques: Models, features and extraction schemes," Med. Image Anal. **13**(6), 819–845 (2009).
[14]R. Klingebiel, E. Siebert, S. Diekmann, E. Wiener, F. Masuhr, M. Wagner, H.-C. Bauknecht, M. Dewey, and G. Bohner, "4-D Imaging in cerebrovascular disorders by using 320-slice CT: Feasibility and preliminary clinical experience," Acad. Radiol. **16**(2), 123–129 (2009).
[15]E. Siebert, G. Bohner, M. Dewey, F. Masuhr, K. T. Hoffmann, J. Mews, F. Engelken, H. C. Bauknecht, S. Diekmann, and R. Klingebiel, "320-slice CT neuroimaging: Initial clinical experience and image quality evaluation," Br. J. Radiol. **82**(979), 561–570 (2009).
[16]N. Yahyavi-Firouz-Abadi, B. L. Wynn, F. J. Rybicki, M. L. Steigner, A. Z. Hussain, R. Mather, E. H. Hanson, M. Ansarinia, and W. W. Orrison, "Steroid-responsive large vessel vasculitis: Application of whole-brain 320-detector row dynamic volume CT angiography and perfusion," AJNR Am. J. Neuroradiol. **30**(7), 1409–1411 (2009).
[17]K. Murayama, K. Katada, M. Nakane, H. Toyama, H. Anno, M. Hayakawa, D. S. M. Ruiz, and K. J. Murphy, "Whole-brain perfusion CT performed with a prototype 256-detector row CT system: Initial experience," Radiology **250**(1), 202–211 (2009).
[18]E. J. Salomon, J. Barfett, P. W. A. Willems, S. Geibprasert, S. Bacigaluppi, and T. Krings, "Dynamic CT angiography and CT perfusion employing a 320-detector row CT: Protocol and current clinical applications," Clinical Neuroradiology **19**(3), 187–196 (2009).
[19]H. A. F. Gratama van Andel, H. W. Venema, C. B. Majoie, G. J. D. Heeten, C. A. Grimber-gen, and G. J. Streekstra, "Intracranial CT angiography obtained from a cerebral CT perfusion examination," Med. Phys. **36**(4), 1074–1085 (2009).
[20]M. Bock, S. O. Schoenberg, F. Floemer, and L. R. Schad, "Separation of arteries and veins in 3D MR angiography using correlation analysis," Magn. Reson. Med. **43**(3), 481–487 (2000).
[21]L. Tianhu, J. K. Udupa, P. K. Saha, and D. Odhner, "Artery-vein separation via MRA—An image processing approach," IEEE Trans. Med. Imaging **20**(8), 689–703 (2001).
[22]C. M. van Bemmel, L. J. Spreeuwers, M. A. Viergever, and W. J. Niessen, "Level-set-based artery-vein separation in blood pool agent CE-MR angiograms," IEEE Trans. Med. Imaging **22**(10), 1224–1234 (2003).
[23]K. Kudo, S. Terae, C. Katoh, M. Oka, T. Shiga, N. Tamaki, and K. Miyasaka, "Quantitative cerebral blood flow measurement with dynamic perfusion CT using the vascular-pixel elimination method: Comparison with h2(15)o positron emission tomography," AJNR Am. J. Neuroradiol. **24**(3), 419–426 (2003).
[24]E. Siebert, G. Bohner, M. Dewey, K. T. Hoffmann, J. Mews, F. Engelken, H. C. Bauknecht, C. Diekmann, F. Masuhr, and R. Klingebiel, "Letter to the editor concerning '320-slice CT neuroimaging: Initial clinical experience and image quality evaluation' [Siebert *et al.*, Br. J. Radiol. **82**(5), 61–70 (2009)]," Br. J. Radiol. **82**(979), 615 (2009).
[25]S. Klein, M. Staring, K. Murphy, M. A. Viergever, and J. Pluim, "Elastix: A toolbox for intensity-based medical image registration," IEEE Trans. Med. Imaging **29**(1), 196–205 (2010).
[26]J. Blom, B. M. ter Haar Romeny, A. Bel, and J. J. Koenderink, "Spatial derivatives and the propagation of noise in Gaussian scale space," J. Visual Commun. Image Represent **4**(1), 1–13 (1993).